Vacuum lifetime and surface charge limit investigations concerning high intensity spin-polarized photoinjectors

Journal of Physics: Conference Series **1350** (2019) 012045 doi:10.1088/1742-6596/1350/1/012045

Vacuum lifetime and surface charge limit investigations concerning high intensity spin-polarized photoinjectors

S Friederich[1], K Aulenbacher[1,2,3] and C Matejcek[1]

[1]Institut für Kernphysik, Johannes Gutenberg-Universität Mainz, Germany
[2]Helmholtz Institute Mainz, Germany
[3]GSI Helmholtzzentrum für Schwerionenforschung, Darmstadt, Germany

E-mail: sifriede@uni-mainz.de

Abstract. The Small Thermalized Electron Source at Mainz (STEAM) is a dc photoemission source. It is designed to operate at up to 200 kV bias voltage with an accelerating field of up to $5\,\mathrm{MV\,m^{-1}}$ at the cathode surface. In several experiments, the properties of GaAs operating under the conditions of spin-polarized photoemission were investigated. Its performance, quantum efficiency lifetime and surface charge limit observations for bulk-GaAs will be discussed.

1. Introduction

The Mainz Energy-Recovering Superconducting Accelerator (MESA) will be built at the Institute for Nuclear Physics at the Johannes Gutenberg University in Mainz [1]. MESA shall operate from 1 mA to 10 mA CW in an energy-recovery mode for the MAGIX [2] and with 150 µA spin-polarized electrons for the P2 [3] experiment. Achieving high currents while staying at low emittances called for the development of a new source with a high extracting field.

2. Source Design

A basic CAD model of STEAM is shown in Fig. 1. It is based on the designs of the Mainzer Microtron (MAMI) [4] dc photoemission source and the inverted insulator design used at the CEBAF source at the Jefferson Laboratory (JLAB) [5]. While the latter design allowed to design a very compact source, the vertical design of the MAMI source was adopted for reasons of cylindrical symmetry. Fourteen $400\,\mathrm{L\,s^{-1}}$ NEG modules gathered around the cathode anode gap of $d = 37\,\mathrm{mm}$ and a $150\,\mathrm{L\,s^{-1}}$ IGP allow to reach a base pressure of around $5 \times 10^{-12}\,\mathrm{mbar}$ after a baking-out period of 300 h at 220 °C.

The photocathodes are prepared in an ultra-high vacuum chamber and transferred to the source through a valve without breaking the vacuum (load-lock operation). The photocathode material is a bulk-GaAs crystal, which is heavily p-doped with zinc atoms, $N_\mathrm{a} \approx 10^{-19}\,\mathrm{cm^{-3}}$. The surface orientation is (100) and its thickness is 500 µm. It is placed in a molybdenum holder in a slice of $11 \times 11\,\mathrm{mm}$ fixed with a tungsten wire spring. The photocathode is heated up to approx. 580 °C for 1 h and prepared with CsO after a 45 min cool-down. By placing a mask in front of the cathode during activation, the deposition of CsO is restricted to a circular area

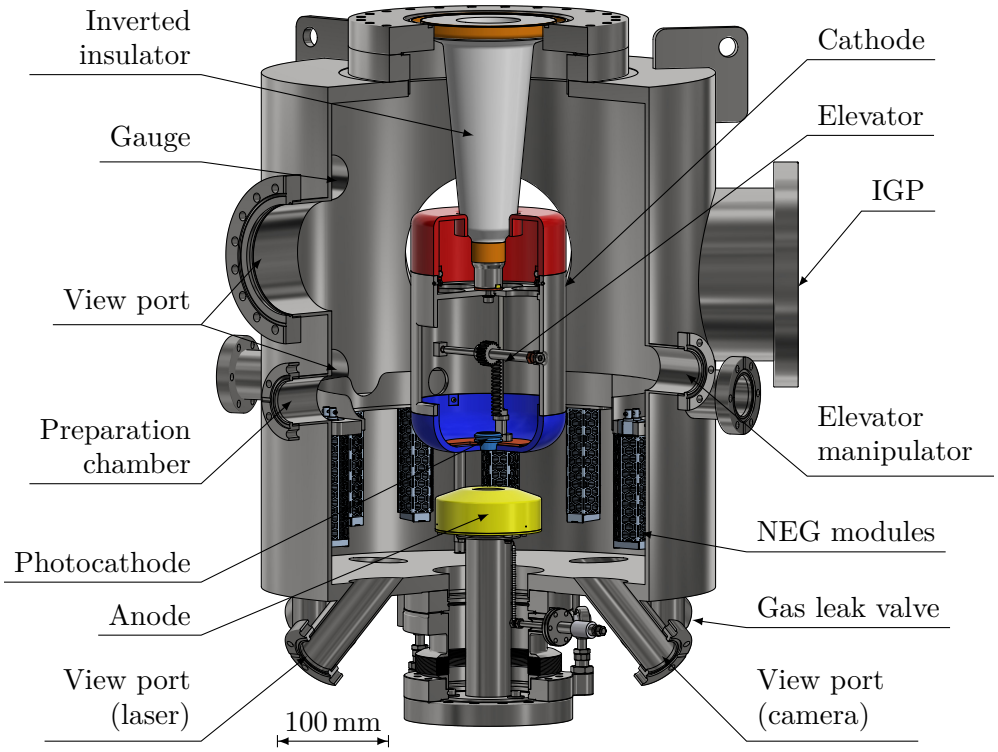

Figure 1. CAD model of the STEAM including the inverted insulator, cathode, potential-free anode and NEG modules.

3 mm in diameter around the center. This technique suppresses the photoexcitation of electrons by stray light.

3. Experimental Set-up

3.1. The laser system

A fibre-coupled laser diode was used as a drive laser and focused on the photocathode through a sideways view port under at an angle of 40°. The wavelength λ_L is 808 nm as needed for the emission of spin-polarized electrons. The maximum laser power P_{max} is 5 W. The elliptical laser spot was measured on a camera sensor. Its root mean square semi-major axis is $\sigma_x = 560\,\mu m$ and its semi-minor axis is $\sigma_y = 780\,\mu m$, resulting in an elliptic area of $A = 1.4\,mm^2$. The quantum efficiencies in the source were measured in the low-laser power regime for dc currents below 20 µA.

3.2. The MELBA

The measurements were performed at the first part of the Mesa Low-energy Beam Apparatus (MELBA) [6], where STEAM is attached to operate at an electron energy of 100 keV resulting in an extraction field of $2.5\,MV\,m^{-1}$. This stage of MELBA consists of a magnetic guiding system, a vacuum system (including a differential pumping stage), diagnostic elements and beam dump. To obtain the results below, the source was operated with pulses at low repetition rates. With respect to beam dynamics in vacuum, and also regarding the dynamics of the surface charge limit effect, the 0.4 ms long pulses create a steady state and therefore correspond to the situation one would meet in regular MESA operation. The low duty cycle is only chosen to mitigate the cathode-damage that is created by gas desorption from the beam dump.

4. Measurements and discussion

4.1. Vacuum lifetime

The quantum efficiency of a photocathode $QE(t)$ is a time-dependent quantity. After a certain time period following the preparation process, an exponential decay in the form of Eq. (1) can be observed.

$$QE(t) = QE_0\, e^{-\frac{t}{\tau}} \text{ with } \frac{1}{\tau} = \frac{1}{\tau_{\text{vac}}} + \frac{1}{\tau_{\text{fe}}} + \frac{1}{\tau_{\text{db}}} \tag{1}$$

Equation (1) introduces the concept of the quantum efficiency lifetime τ. It depends on multiple uncorrelated factors.

The vacuum lifetime τ_{vac} is always present as residual gas in the source chamber reacts with the CsO layer on the photocathode surface, leading to its disintegration. Hence, the source vacuum has to be as good as possible. Parasitic field emission, τ_{fe}, can occur just by applying the high voltage to the cathode and τ_{db} is the lifetime due to gas desorption resulting from the electrons hitting the beam line or the dump.

Figure 2 shows two measured vacuum lifetimes. Compared to the rather short lifetime of $\tau_{\text{vacuum}}^{\text{prep chamber}} = 52\,\text{h}$ measured in the preparation chamber, the lifetime inside the source $\tau_{\text{vacuum}}^{\text{STEAM}} = 3170\,\text{h}$ is enlarged by a factor of 61.

The effect of field emission, τ_{fe}, is negligible as the source was high-voltage processed with residual gas. Afterwards no sign of field emission was detected. The lower plot of Fig. 2 indicates multiple lifetime reducing events dominated by the mentioned gas desorption of the beam dump.

4.2. Surface charge limit

When illuminating NEA GaAs with high intensity laser light, one can observe a saturation effect of the emitted current, i. e. the number of emitted electrons does not increase linearly with the laser power. This effect was first observed for GaAs at SLAC [7] and is called *surface charge limit*.

A scheme is shown in Fig. 3: Photoexcited electrons in NEA GaAs diffuse to the surface. On their way, they scatter with optical phonons, lose energy (thermalization) and may recombine with holes. Electrons that reach the surface may tunnel to the vacuum, contributing to the measured electron yield, or get trapped in the band bending region. The trapped electrons compensate for the positive charge in the surface states and build up a repulsive Coulomb potential leading to a *surface photovoltage* U_{SPV} that reduces the NEA χ. In contrast to this, the accelerating field of the source lowers the potential barrier by δU (Schottky effect). A current of holes tunnelling from the valence band into the surface helps restoring the default potential situation.

Figure 4 shows some measurements done at high currents of up to 10 mA, limited by the power supply. The surface charge limit effect was observed. Measurements ① to ③ were taken rather shortly after a fresh preparation when the quantum efficiency was above 1 %. Measurements ④ to ⑥ were conducted after several lifetimes including high-current experiments. The quantum efficiency is below 0.9 % for these measurements.

Following the capacitor-like approach by Mulhollan et al. [8], who described the effect for thin layered GaAs photocathodes, the results were fitted with Eq. (2):

$$\frac{I_{\text{e}}}{A} = QE_0\, \frac{\lambda_{\text{L}}}{hc}\, \frac{P}{A} \left[1 - \frac{E_0}{\widetilde{\chi}}\, \ln\left(1 + \frac{QE_0}{j_{\text{p}}}\, \frac{\lambda_{\text{L}}}{hc}\, \frac{P}{A}\right)\right] \tag{2}$$

Here $E_0/\widetilde{\chi} = E_0/(|\chi + \delta U|)$ is the ratio between hole surface barrier E_0 that suppresses the hole current and the electron affinity[1] $\chi = (-15 \pm 4)\,\text{meV}$ which is lowered by the extracting

[1] χ is a mean value extracted from two QE-vs-$\sqrt{U}$-fits taken after a fresh preparation as done in [8].

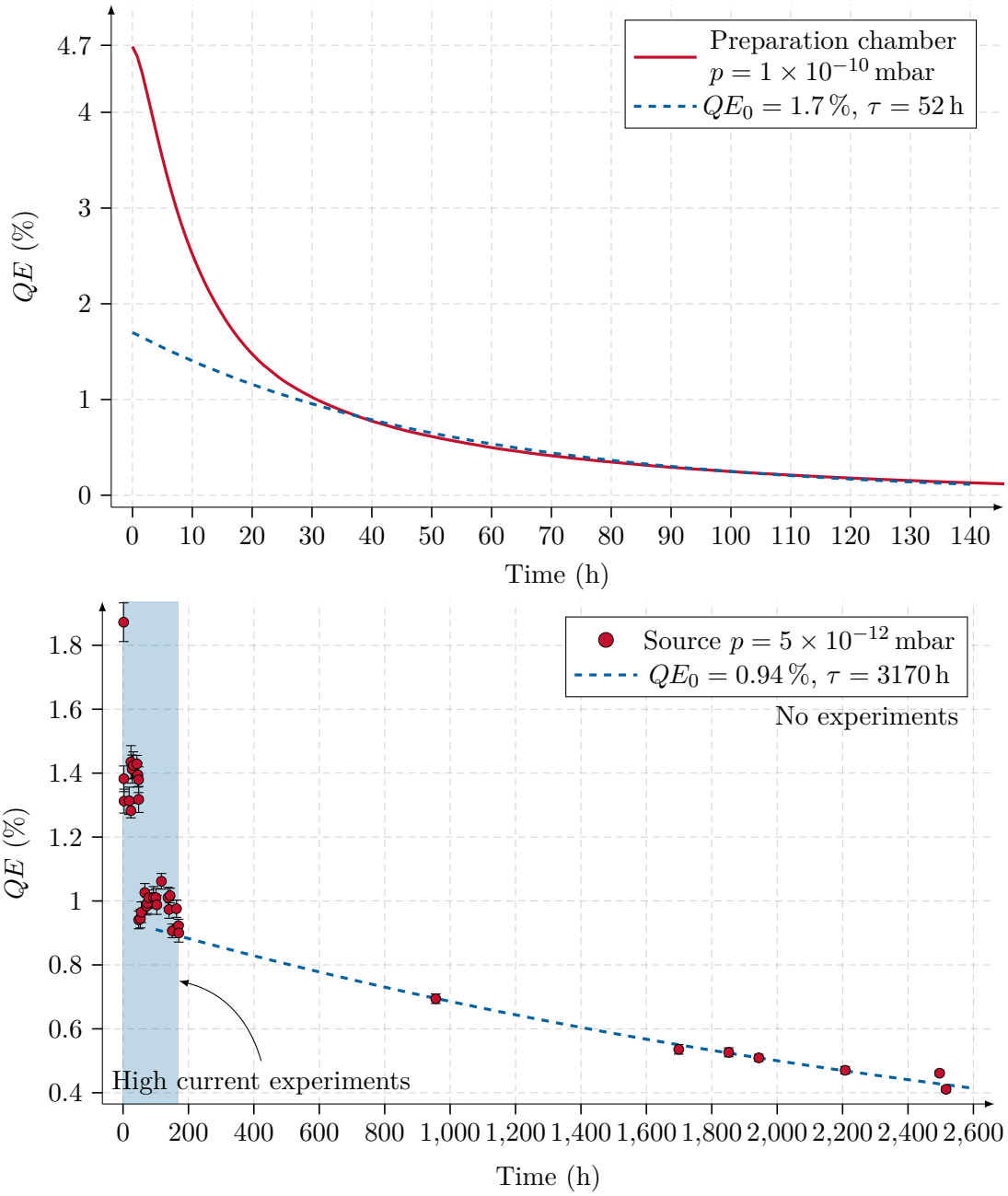

Figure 2. Lifetime measurements. (Top) measurement in the preparation chamber: Current measured every 15 min, laser power on cathode 100 µW with the full illumination of 3 mm active CsO layer. (Bottom) Measurement at STEAM with 1.4 mm^2 elliptical laser spot at low laser intensities.

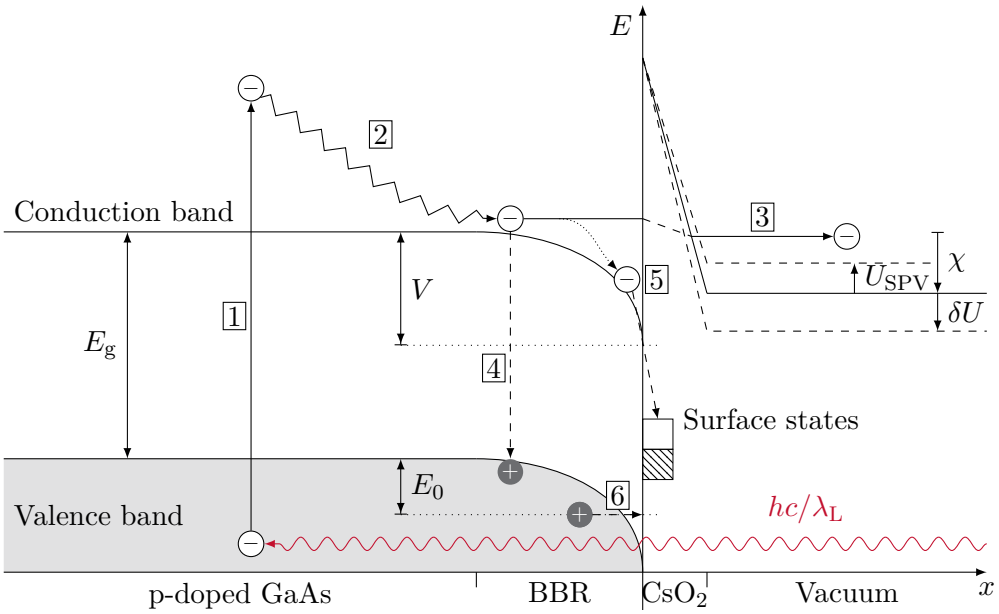

Figure 3. Simplified scheme of the energy levels on the surface of a p-doped bulk-GaAs with negative electron affinity (NEA) due to a CsO layer without image force correction. [1] Photoexcitation; [2] Thermalization and diffusion to the surface; [3] Tunnelling through surface barrier and measurable electron yield; [4] Recombination to valence band; [5] Trapping of electrons in band bending region (BBR) and recombination with holes; [6] Tunneling of holes into the surface states.

field by $\delta U(2.5\,\mathrm{MV\,m^{-1}}) = -55\,\mathrm{meV}$ as indicated in Fig. 3. j_p is the hole current density tunneling to the surface and QE_0 is the quantum efficiency as if there was no charge limit effect. The parameters E_0 und j_p are given by:

$$E_0 = E_{00}\coth\left(\frac{E_{00}}{kT}\right) \text{ with } E_{00} = \frac{\hbar}{2}\sqrt{\frac{e^2 N_a}{m_\mathrm{h}\epsilon_0\epsilon_s}} \tag{3}$$

$$j_\mathrm{p} = A^* \frac{T\sqrt{E_{00}V}}{k\cosh(E_{00}/kT)} \exp\left(-\frac{V}{E_0}\right) \tag{4}$$

Following [8], the theoretical values for metal-semiconductor junctions are calculated from [9] through Eq. (3) and Eq. (4), where m_h is the hole mass, e is the electrical charge, N_a is the acceptor concentration, ϵ_0 is the vacuum permittivity, $\epsilon_s = 13$ is the permittivity of GaAs, k is the Boltzmann constant. $A^* = 4\pi m_\mathrm{h} e k^2/h^3$ is the effective Richardson constant for holes.

The results of fitting Eq. (2) to the measurements in Fig. 4 are listed in Table 1. The mean value of the energy barrier is $\langle E_0\rangle = (25 \pm 3)\,\mathrm{meV}$. This value lies below the theoretical barrier height at room temperature ($kT = 25\,\mathrm{meV}$) of 32 meV and 59 meV for heavy and light holes respectively.

The mean of the recovering hole current is $\langle j_\mathrm{p}\rangle = (0.30 \pm 0.08)\,\mathrm{A\,cm^{-2}}$. Assuming the restoring current is dominated by light holes, $\langle E_0\rangle$ and this value result in an initial band bending well, shown in Fig. 3, of $V = 0.40\,\mathrm{eV}$ and hence V is approximately 28 % of the band gap energy $E_\mathrm{g} = 1.42\,\mathrm{eV}$.

The extrapolation of curve ① in Fig. 4 indicates that a saturated current density of $1\,\mathrm{A\,cm^{-2}}$ could have been reached at 808 nm with bulk-GaAs. The surface charge limit

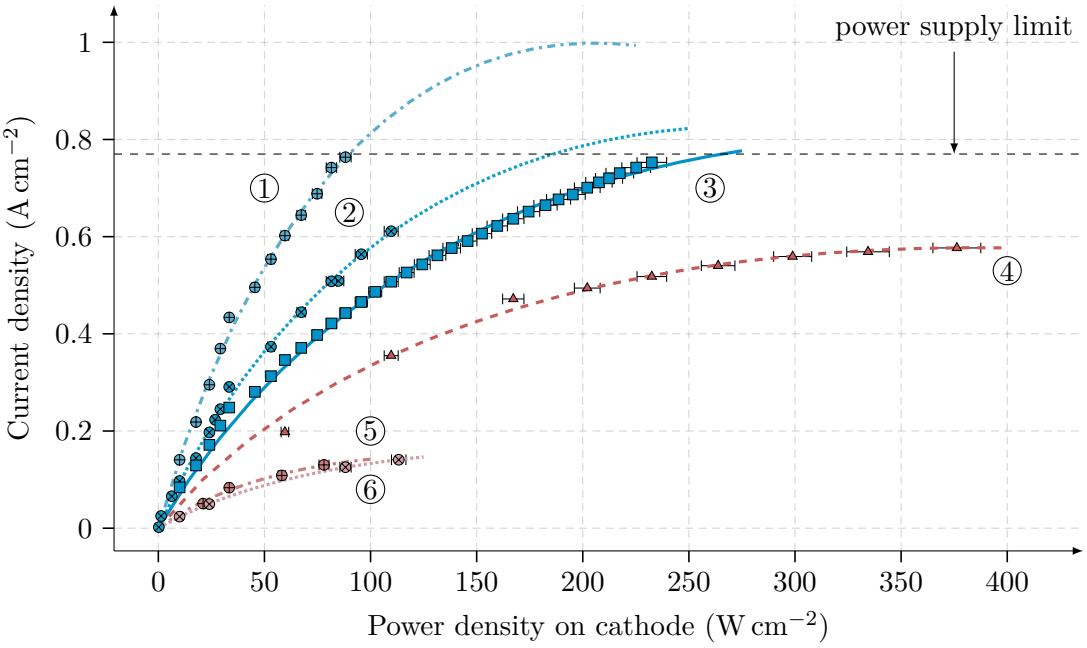

Figure 4. The charge limit effect for bulk-GaAs measured at STEAM. The colors blue and red indicate the same photocathode but after different preparations between the measurements.

Table 1. Fit Results for the Charge Limit Measurements

No.	QE_0	$E_0/\tilde{\chi}$	E_0 (meV)	j_p (A cm^{-2})
①	2.40 %	37 %	26	0.58
②	1.55 %	34 %	24	0.39
③	1.15 %	35 %	25	0.41
④	0.85 %	30 %	21	0.20
⑤	0.50 %	40 %	28	0.11
⑥	0.39 %	39 %	28	0.10

restricts the space charge limitation given by the one-dimensional Child-Langmuir limit $j_\mathrm{e,cl} = 2.33 \times 10^{-6}\, U^{3/2}/d^2 = 5.4\,\mathrm{A\,cm^{-2}}$ below 20 %.

5. Summary and outlook

High current experiments with NEA bulk-GaAs were done at the new photoemission electron source STEAM, achieving MESA stage 2 parameter. The charge limit effect was observed, so currents above 10 mA can be reached if the quantum efficiency stays above 1 % in the infrared wavelength regime. Higher values should be achievable with gradient doped cathodes such as strained superlattices with a doping level of $5 \times 10^{19}\,\mathrm{cm^{-1}}$ in the surface region [10]. For a quantum efficiency below 1 %, the achievable current density is also below 13 % of the space charge limitation. Hence, it is essential to enlarge the photocathode lifetime. One measure is a very low vacuum as present in STEAM, reaching multiple thousands of hours vacuum lifetime.

Acknowledgments
This work is supported by the DFG excellence initiative PRISMA+ and by the German Federal Ministry of Education and Research through "Verbundforschung FKZ 05K16UMA" (the HOPE-2 joint project).

References
[1] Hug F, Aulenbacher K, Heine R, Ledroit B and Simon D 2017 MESA - an ERL Project for Particle Physics Experiments *Proc. of Linear Accelerator Conference (LINAC'16), East Lansing, MI, USA, 25-30 September 2016* (*Linear Accelerator Conference* no 28) (JACoW) pp 313–315
[2] Doria L, Achenbach P, Christmann M, Denig A, Gülker P and Merkel H 2018 Search for light dark matter with the MESA accelerator *13th Conference on the Intersections of Particle and Nuclear Physics (CIPANP 2018)*
[3] Becker D, Bucoveanu R, Grzesik C, Kempf R, Imai K, Molitor M, Tyukin A, Zimmermann M, Armstrong D, Aulenbacher K *et al.* 2018 *The European Physical Journal A* **54**(208)
[4] Aulenbacher K, Nachtigall C, Andresen H G, Bermuth J, Dombo T, Drescher P, Euteneuer H, Fischer H, Harrach D, Hartmann P, Hoffmann J, Jennewein P, Kaiser K H, Köbis S, Kreidel H J, Langbein J, Petri M, Plützer S, Reichert E, Schemies M, Schöpe H J, Steffens K H, Steigerwald M, Trautner H and Weis T 1997 *Nuclear Instruments and Methods in Physics Research Section A: Accelerators, Spectrometers, Detectors and Associated Equipment* **391** 498–506
[5] Adderley P A, Clark J, Grames J, Hansknecht J, Surles-Law K, Machie D, Poelker M, Stutzman M L and Suleiman R 2010 *Physical Review Special Topics Accelerators and Beams* **13**(1)
[6] Matejcek C, Aulenbacher K and Friederich S 2019 Low Energy Beam Transport System for MESA *Proc. 10th Int. Particle Accelerator Conf. (IPAC'19)* TUPGW028
[7] Woods M, Clendenin J, Frisch J, Kulikov A, Saez P, Schultz D, Turner J, Witte K and Zolotorev M 1993 *Journal of Applied Physics* **73** 8531–8535
[8] Mulhollan G A, Subashiev A V, Clendenin J E, Garwin E L, Kirby R E, Maruyama T and Prepost R 2001 *Physics Letters A* **282**(4–5) 309–318
[9] Padovani F A and Stratton R 1966 *Solid-State Electronics* **9** 695–707
[10] Maruyama T, Brachmann A, Clendenin J, Desikan T, Garwin E, Kirby R, Luh D A, Turner J and Prepost R 2002 *Nuclear Instruments and Methods in Physics Research Section A: Accelerators, Spectrometers, Detectors and Associated Equipment* **492** 199–211